HOSTED BY
ELSEVIER
Available online at www.sciencedirect.com
ScienceDirect
International Soil and Water Conservation Research 3 (2015) 305–315
www.elsevier.com/locate/iswcr

Identification of potential soil water retention using hydric numerical model at arid regions by land-use changes

Mohamed Abu-hashim[a,*], Elsayed Mohamed[b], Abd-ElAziz Belal[b]

[a]*Soil Science Department, Zagazig University, Zagazig, 44511, Egypt*
[b]*National Authority for Remote Sensing and Space Sciences (NARSS), Cairo, 19765, Egypt*

Received 28 August 2015; received in revised form 28 October 2015; accepted 29 October 2015
Available online 10 November 2015

Abstract

Assessment of soil water retention in arid region is an input required parameter in precision water management at large scale. Investigations were carried out in Tanta catchment in the middle Nile Delta, Egypt (30° 45 N, 30° 55 E), where collecting soil samples covered different hydrological soil groups and land-uses. Based on the natural resource conservation service curve number model (NRCS-CN), CN approach was used to investigate the effect of spatio-temporal variations of different land-uses on soil water retention. Potential soil water retention from 1990 to 2015 was reduced by 118.1 m^3 per hectare with decreasing cropland area. Urbanization encroachment from 1990 to 2015 was increased by 2.13% by decreasing cropland with 15.3% (5300 ha in 2015). This resulted in losing the potential soil water retention by 625,968.42 m^3 water for the whole catchment area. Impact of land degradation was pronounced, where 2.65%, 29.35%, and 1.11% of the initial crop land-use in 1990 were converted to bare soil, fallow, and urban area, respectively in 2015. Implementation of (*S*) value of the NRCS-CN model with GIS technique provides useful measure to identify land-use changes of potential water storage capacity at catchment scale.
© 2015 International Research and Training Center on Erosion and Sedimentation and China Water and Power Press. Production and Hosting by Elsevier B.V. This is an open access article under the CC BY-NC-ND license (http://creativecommons.org/licenses/by-nc-nd/4.0/).

Keywords: Curve number model; Land-use; Potential water retention; Spatio-temporal variations

1. Introduction

Land-use changes are important parameters in the runoff process as they affect water storage capacity in the Mediterranean regions. These changes resulted from agriculture intensification, people relocation in urban areas, grazing abandonment inland, and explosion in urbanization (Brandt & Thornes, 1996; Drake & Vafeidis, 2004). Monitoring these changes required accurate spatio-temporal land-use/land cover (LULC) mapping over large areas that become operationally available by multispectral satellite data. In fact such data sets facilitate monitoring processes of LULC and urbanization change studies due to its accurate spectral resolution. Land degradation reflects

*Corresponding author. Tel.: +20 1156621010; fax: +20 552287567.
E-mail address: mohamed.abu-hashim@gmx.de (M. Abu-hashim).
Peer review under responsibility of IRTCES and CWPP.

http://dx.doi.org/10.1016/j.iswcr.2015.10.005
2095-6339/© 2015 International Research and Training Center on Erosion and Sedimentation and China Water and Power Press. Production and Hosting by Elsevier B.V. This is an open access article under the CC BY-NC-ND license (http://creativecommons.org/licenses/by-nc-nd/4.0/).

the well-tendency of soil to surface runoff (Sharma, 1998; Kosmas, Danalatos, & Gerontidis, 2000). Removing vegetation covers with increasing urbanization leads to an increase in overland flow and surface runoff. Surface runoff, a subsidiary parameter of soil degradation, was determined using natural resource conservation service—curve number model (Hawkins, Ward, Woodward, & Van Mullem, 2009). Due to its simplicity, curve number (CN) model was used by the hydrologists of US Soil Conservation Service (SCS) to identify the direct surface runoff in ungauged agricultural basins and for non-agricultural watersheds (Ponce & Hawkins 1996; Mishra & Singh, 2006). CN is a dimensionless value, which has been identified experimentally for a variety of different soil, land-use, land management situations, and hydrologic conditions for small scale catchments in US. In addition, CN is related to the retention soil water potential (S) and the curve number model considers many factors including land-use change, soil type, land management, treatment, antecedent soil moisture condition, and surface condition (Hawkins, 1993; Michel, Andréassian, & Perrin, 2005). Therefore, this methodology is well-grasped and well established in documenting the environmental features (Chow, Maidment, & Mays, 1988; Romero, Castro, Gomez, & Fereres, 2007; King, & Balogh, 2008). Although CN model was mainly developed for identifying runoff in agricultural basins, it is adopted for several land-uses as well as urbanized watersheds (Mishra & Singh, 2006), and its scope extended to be an integral parameter of complex and simulation water retention models (Lyon, Walter, Gerard-Marchant, & Steenhuis, 2004; Zhan & Huang, 2004; Mishra, Geetha, Rastogi, & Pandey, 2005; Soulis & Dercas, 2007; Geetha, Mishra, Eldho, Rastogi, & Pandey, 2008; Singh, Bhunya, Mishra, & Chaube, 2008). CN has experimentally been identified for different LULC situations for small catchments to determine the actual and/or potential water retention and direct surface runoff (Romero et al., 2007; Hawkins et al., 2009). In addition, Mantey and Tagoe (2013) reported that the hydrologic soil groups (HSGs), land use and DEM were the main parameters used to generate curve number value. Geographical information system (GIS) was performed as an efficient technique for preparation of input date required by the SCS curve number model (Latha, Rajendran, & Murugappan, 2012, 2012). Curve number value can be established from remote sensing digital data by correlating generalized LULC with hydrologic soil groups and the tables that were presented by the SCS and experimentally identified (Zhan & Huang 2004). In addition, remote sensing immensely helps in rapid identification of LULC that is used as an input tool in the SCS model (Kumar, Tiwari, & Pal, 1991; Chen, Wang, Pollino, & Merrin, 2012).

Water requirements in Nile Delta are continuously rising due to population growth and enhancing standards of living (Mohamed & Belal, 2015). Annually, agricultural sector that consumes the largest component of total water demand, exhausts more than 85% of Egypt's portion of the Nile water. Water issue in Nile Delta is rapidly considering alarming proportion, that by the year 2020, Egypt will lose 20 percent more water of its share. With this loosening grip on Egyptian Nile portion, water scarcity would endanger the country's stability (MWRIE, 2014), resulting in land degradation processes, that has widely been recognized (Kosmas et al., 2000). This phenomenon resulted from drought, poor agricultural practices, deterioration of vegetation cover, soil organic matter losses, and reduction of its soil water storage that would result in soil desertification (Thornes, 1985).

The objective of this work is to integrate soil, remote sense data, GIS and hydrological model to map soil water retention in arid region for precision water management. Specific objectives included study of spatio-temporal variations of LULC and their effects on the potential water retention in a Nile Delta region.

2. Material and methods

2.1. Experimental site

Investigations were carried out in the middle of Nile Delta at the catchment area of Tanta (30° 45′ N, 30° 55′ E), that was aligned by Damietta and Rosetta branches as shown in Fig. 1. The catchment area is 34,650 ha and has a maximum altitude of 40 m above sea level (asl). The studied area is characterized by Mediterranean climatic conditions with seasonal and spatial variations of rainfall and high oscillations in daily temperatures. Climatic data of Tanta Meteorological Station (TMS, 1960–2010) indicate 45.1 mm annual rainfall for Tanta city that falls mainly in the winter seasons. Mean of annual and maximum temperature was 20.1 and 45.7 °C. Central part of Nile Delta is classified by sedimentary non-consolidated deposits belonging to the quaternary area that is differentiated into four different deposits: young deltaic, Fluvio-marine, young Eolian, and old Eolian.

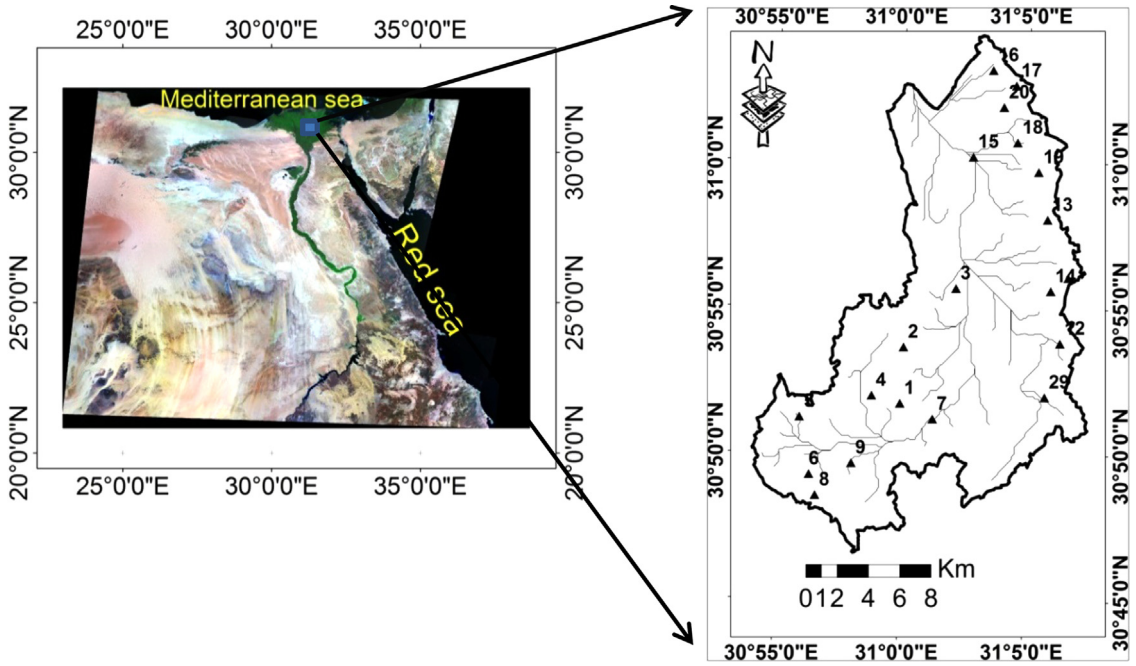

Fig. 1. Location of the studied catchment area in the Mediterranean region.

2.2. Digital image processing

Datasets of the studied area were acquired using Landsat7 Enhanced Thematic Mapper (ETM+7) in May 1990 and Landsat 8 with spatial resolution 30 m in May 2015. The scenes were selected to be geometrically corrected and calibrated. Digital elevation model (DEM) with 30×30 m^2 resolution, and elevation points were recorded during the field survey by GPS (Fig. 2).

2.3. Land use and land cover changes

Using multi-temporal classification, change detection in LULC from 1990 to 2015 was determined by specification of joint models. Post-classification technique was used as the most efficient method. Support vector machine (SVM) was used to determine LULC changes that were applied on the images taken in 1990 and 2015. SVM classifier was turned out to be a representative method for the complex distributions of LULC that are identified in the studied area at several spatial resolution scales. For this area, SVM classifier provides four types of kernels (Chen, Stow, & Gong, 2004; Mountrakis, Im, & Ogole, 2011), in which neighboring pixels were characterized and signed in classes as agriculture, fallow, bare soil, water, and urban area.

2.4. Catchment delineation and soil sampling criteria

Catchment delineation was performed using DEM, representing site morphological properties, that is considered a standard routine in most geographic information systems (GIS) techniques. Before carrying out hydrological computations, hydrological correctness of DEM was prepared. The terrain models always contain small errors arisen from their production (different input data and laser scanning digitized contour lines) which will produce artefacts. As a final step, real stream data were overlaid upon the generated catchments in order to identify the sub-catchments that contribute to a single stream (Fig.1). Several soil samples were collected during spring season in Tanta catchment in 2015 (Fig.1). Suitable sampling sites were identified by computing hydrologic soil groups (HSG), soil type, land management, surface hydrologic conditions, and the region land-uses and combining them to hydrologic response units (HRU_s) in GIS. The fields were under conventional farming management (CM) of monoculture

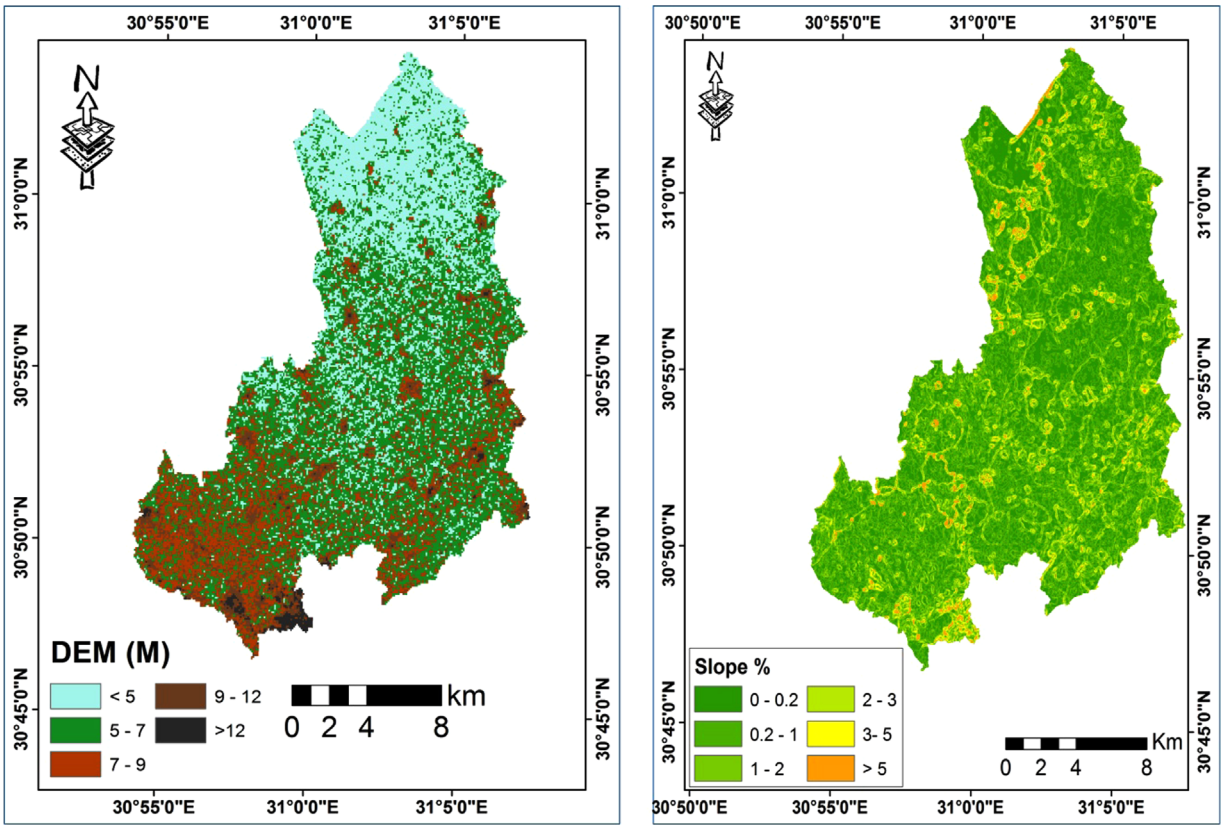

Fig. 2. Digital elevation model and the slope distribution at the catchment area.

cultivations with conventional tillage and removal of crop residues after harvest. Twenty sample locations were selected using HRU_s that cover different land-use, soil types, and HSG of the catchment. Soil physical analyzes at Tanta catchment were investigated according to Klute, 1986 (Table 1). Pedo-transfer functions (Saxton, Rawls, Romberger, & Papendick, 1986) were used to compute soil properties (e.g. saturated hydraulic conductivity *Ks*) based on their textural composition.

2.5. Soil water retention computation

The relation of the soil water retention S to the curve number (CN) value is shown in the following equations:

$$S = (25,400/CN) - 254 \quad (1)$$

where S is the soil water retention in (mm), and CN is the curve number value (dimensionless). Conceptually, CN can vary from 0 to 100, that is corresponding to $S = \infty$ and $S = 0$ respectively. Using this model requires to identify the curve number value from tables that are based on land management, land-use categories, surface hydrologic conditions, and hydrologic soil groups (SCS, 1972; Natural Resource Conservation Service, 2004; Hawkins et al., 2009). Table 2 displays the curve number handbook (TR 55) that was prepared by (SCS, 1986; NRCS, 2004) and used in the context of this work. In order to determine CN, soils were classified by texture and water transmission (*Ks)* into four hydrologic soil groups (HSGs). HSG A has high rate of water transmission > 18.29 cm d^{-1}, HSG B has moderate rate of water transmission 9.14–18.24 cm d^{-1}, HSG C has low rate of water transmission 3.04–9.14 cm d^{-1}, and HSG D has the lowest rate of water transmission 0.00–3.04 cm d^{-1} (SCS, 1972; NRCS, 2004; Hawkins et al., 2009). Fig. 3 displays the flow chart of modeling GIS technique to identify the spatial distribution of the soil water retention at large scale through hydrological models based on the NRCS-CN method.

Table 1
Soil physical properties for the study area.

Sample ID	Sand %	Silt %	Clay %	Soil texture	B.D. g cm^{-3}	F.C. %	Ks cm d^{-1}	HSG
1	41.08	44.32	14.60	Loam	1.45	25.7	37.9	A
2	33.78	41.23	24.99	Loam	1.43	31.4	13.8	B
3	38.06	36.88	25.02	Loam	1.48	32.1	13.0	B
4	37.93	39.45	22.62	Loam	1.50	30.5	16.4	B
5	39.05	29.67	31.28	Clay Loam	1.52	32.9	7.5	C
6	45.01	34.59	20.40	Loam	1.51	27.4	18.9	A
7	48.57	39.36	12.07	Loam	1.52	22.8	49.3	A
8	37.22	29.68	33.10	Clay Loam	1.48	35.1	6.8	C
9	36.46	23.31	31.23	Clay Loam	1.50	34.8	7.9	C
10	36.56	24.19	39.25	Clay Loam	1.48	38.7	4.7	C
11	33.91	26.86	39.23	Clay Loam	1.42	38.5	5.0	C
12	34.12	21.42	44.46	Clay	1.48	41.1	4.0	C
13	28.57	26.85	44.58	Clay	1.44	41.8	4.4	C
14	31.44	26.78	41.78	Clay	1.45	39.7	4.6	C
15	37.00	21.36	41.64	Clay	1.54	38.8	4.2	C
16	36.66	18.79	44.55	Clay	1.41	39.5	3.8	C
17	31.51	29.43	39.06	Clay Loam	1.50	38.2	5.3	C
18	39.54	21.70	39.06	Clay Loam	1.47	37.8	4.5	C
19	39.89	29.26	30.85	Clay Loam	1.41	34.6	7.7	C
20	41.08	44.32	14.60	Loam	1.55	26.1	37.9	A

B.D.: bulk density, O.M.: organic matter, F.C.: field capacity % vol., Ks: saturated hydraulic conductivity, HSG: Hydrologic soil group

3. Results

3.1. Land-use change for the catchment

Land-use changes from 1990 to 2015 are shown in Table 3 and Fig. 4. Tanta catchment is close to the city of Tanta in the middle of Nile Delta where urban encroachment is the dominating process resulting in a decrease of cropland. Between 1990 and 2015, cropland showed the most representative loss by 15.3% (5300 ha), whereas urban area showed an increase by 2.13 % (Table 3). Bare soil slightly increased by 1.2 % as a result of land degradation in the Middle Delta. To show the dynamics of land-use changes, land-use in 2015 was traced back to its use in 1990. Results are displayed in Table 4. The diagonal of the table shows the stable land-use which stayed the same over the past 25 years. Approximately 66.8% of cropland-use in 1990 still forms crop land-use in current status-quo in 2015. Moreover, the impact of land degradation in Tanta catchment area was pronounced, where 2.65%, 29.35%, and 1.11% of initial crop land-use in 1990 were converted to bare soil, fallow, and urban area, respectively in 2015. It is interesting to compare the absolute change of bare soil and the land-use distribution between 1990 and 2015 (Table 3). The total change has only increased by 1.2%. In the last 25 years, only 27.7% of the bare soil was kept stable (Table 4). Conversion of bare soil to urban area is pronounced in this region where 31.8% of bare soil in 1990 was converted to urban area in 2015. Approximately 82.78% of urban area-use in 1990 still forms urban area in the current status-quo of 2015. Fallow soil exhibited the same trend as 30.2% still forms fallow land use in 2015. Approximately 52.9% of the initial fallow land uses in 1990 were converted to cropland in 2015 (Table 4).

3.2. Potential soil water retention

Soil physical properties for Tanta catchment area showed that the dominant soil types are loamy and clay loam soil (Table 1). Soil field capacity varied from 22.8 to 41.8%, while dry bulk density varied from 1.41 to 1.55 g cm^{-3}. The study area is characterized by flat to gently sloping where the northern part attributed by flat ranging between 0 and 0.2% except some patches, meanwhile the southern part has slope gradient ranging between 0.2 and 1% as shown in Fig. 2.

Table 2
Curve number values extracted from published tables listed in NRCS-CN, 1986 (TR-55) Handbook manual.

Land-use	Treatment	Hydrologic condition	Curve number for hydrologic Soil group			
			HSG A	HSG B	HSG C	HSG D
Bare soil	–	–	77	86	91	94
Fallow	Crop residue cover (CR)	Poor	76	85	90	93
		Good	74	83	88	90
Cropland	Straight row(SR)	Poor	72	81	88	91
		Good	67	78	85	89
Cropland	SR + CR	Poor	71	80	87	90
		Good	64	75	82	85
Cropland	Contoured (C)	Poor	70	79	84	88
		Good	65	75	82	86
Cropland	C + CR	Poor	69	78	83	87
		Good	64	74	81	85
Urban area	–	–	98	98	98	98
Water	–	–	100	100	100	100

Poor: factors impair infiltration and tend to increase runoff.
Good: factors encourage average and better than average infiltration and tend to decrease runoff.

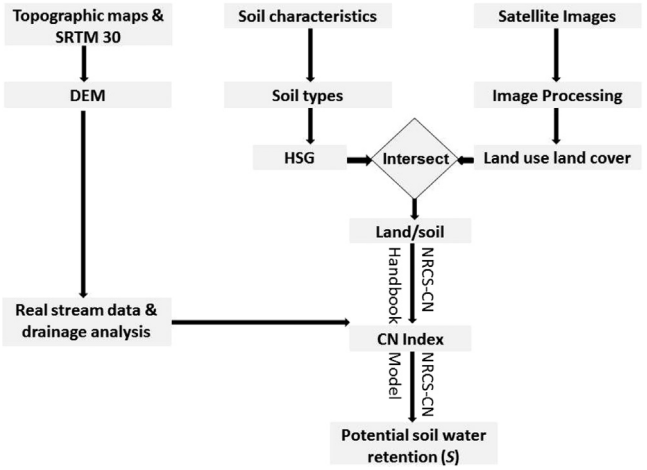

Fig. 3. Flowchart of modeling GIS-based land use to identify the spatial distribution of the soil water retention at large scale coupled with the hydrological models NRCS-CN method.

Table 3
Land-use changes of Tanta catchment area in 1990 and 2015.

Land-use	1990	2015	Change (%)
Cropland	25,810.36	20,510.06	−15.31
Bare soil	1370.62	1786.66	1.20
Fallow	5315.29	9442.29	11.92
Urban area	2028.11	2765.88	2.13
Water	104.68	124.17	0.06

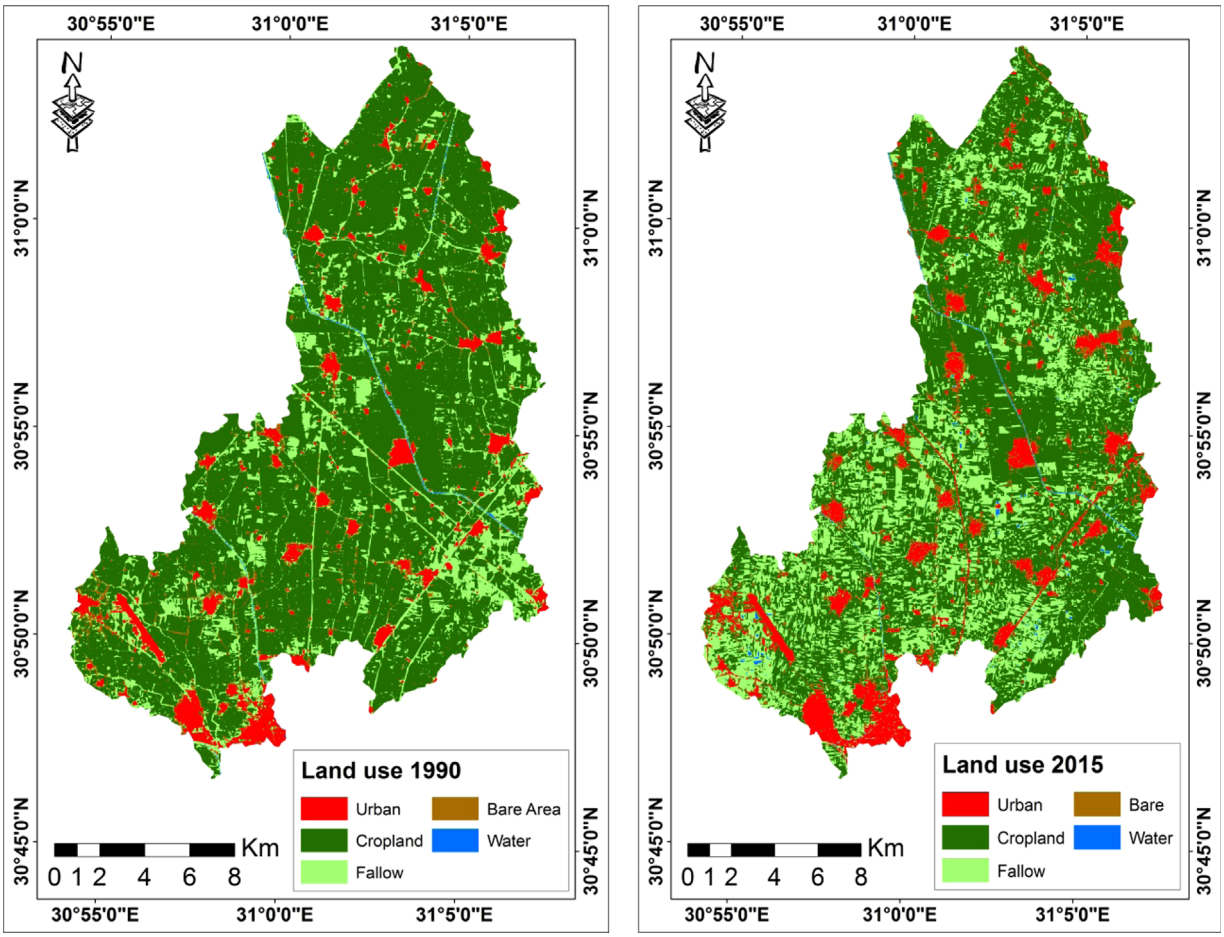

Fig. 4. Spatial distribution of land use in 1990 and 2015 for Tanta catchment area.

Fig. 5 shows spatial distribution of the curve number values for the whole basin. HSG was established for the basin based on analysis of soil parameters as: texture, infiltration, and retention capacity of each pedological unit (Table 2). Results of land-use types of Tanta basin in 2015 were prepared using post-classification technique (Fig. 4). In order to estimate the spatial distribution of the soil water retention for the whole catchment, the LULC maps were conducted with NRCS data in Table 2 to identify the CN values according to the related HSG under each land-use (Fig. 5). The obtained CN maps were then solved by Eq. (1) to compute the spatial distribution of the soil water retention at the whole catchment area for each pedological unit (Fig. 6).

Soil water retention (S) was interpreted in analogy to precipitation in [mm] or [l m^2]. With performing land-use in the catchment in hectares, a retention value of 1 [mm] is equal to 10 [m^3 ha^{-1}]. As the total area of Tanta catchment is 34,329.06 ha, and cropland area decreased from 25,810.36 ha in 1990 to 20,510.06 ha in 2015 (Table 3), the total

Table 4
Distribution percentage of each land-use class in 1990 to the current status 2015 in Tanta catchment area.

1990/2015	Cropland (%)	Bare soil (%)	Fallow (%)	Urban area (%)	Water (%)
Cropland	**66.75**	2.65	29.35	1.11	0.14
Bare soil	27.73	**27.95**	12.42	31.81	0.08
Fallow	52.92	8.71	**30.16**	7.52	0.70
Urban area	2.35	12.41	2.35	**82.78**	0.10
Water	22.39	3.28	34.99	4.81	**34.53**

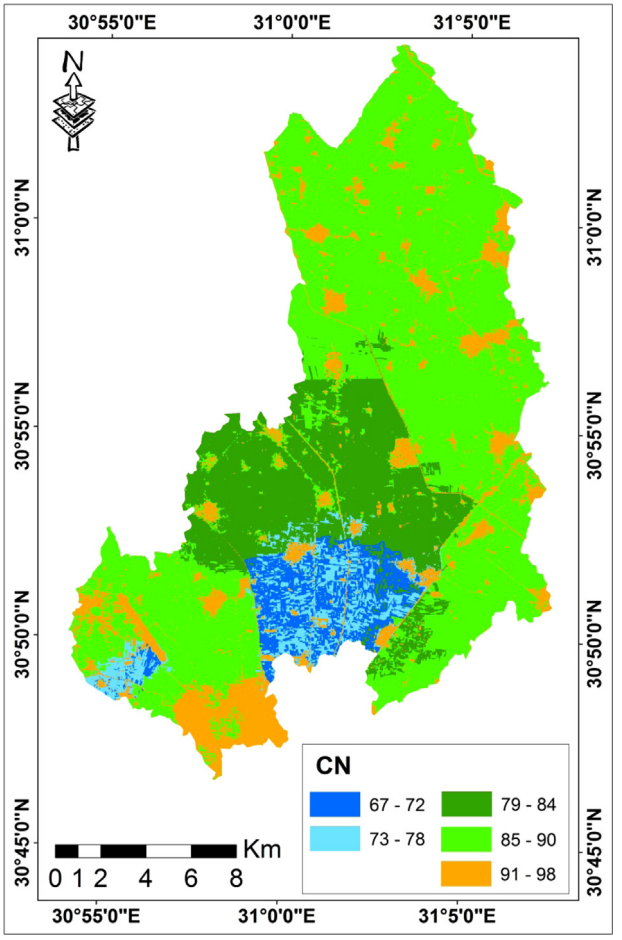

Fig. 5. Curve number distribution at Tanta catchment scale computed by the NRCS-CN model.

soil water retention of cropland area decreased from 57.51 mm to 45.70 mm. Therefore, 118.1 m^3 water per hectare can be lost with decreasing the cropland between 1990 and 2015. Thus, soil water retention from the whole catchment area reveals decreasing the cropland area by 5300 ha in 2015 results in losing 625,968.42 m^3 water of its storage capacity. In addition, the most representative area having higher S that ranged from 106 to 125 mm (4.8% of total) fell in the southern part which retained more water than the other areas in the catchment. These findings were convenient with the field measurements of soil dry bulk density that the highest S values in the southern part of the catchment area correlated with the lowest soil dry bulk density (1.41–1.45 g cm^{-3}) in the study area. While 12.6% of the total area confined to < 25 mm water retention values, the dominant area in the catchment (57.9%) retain water

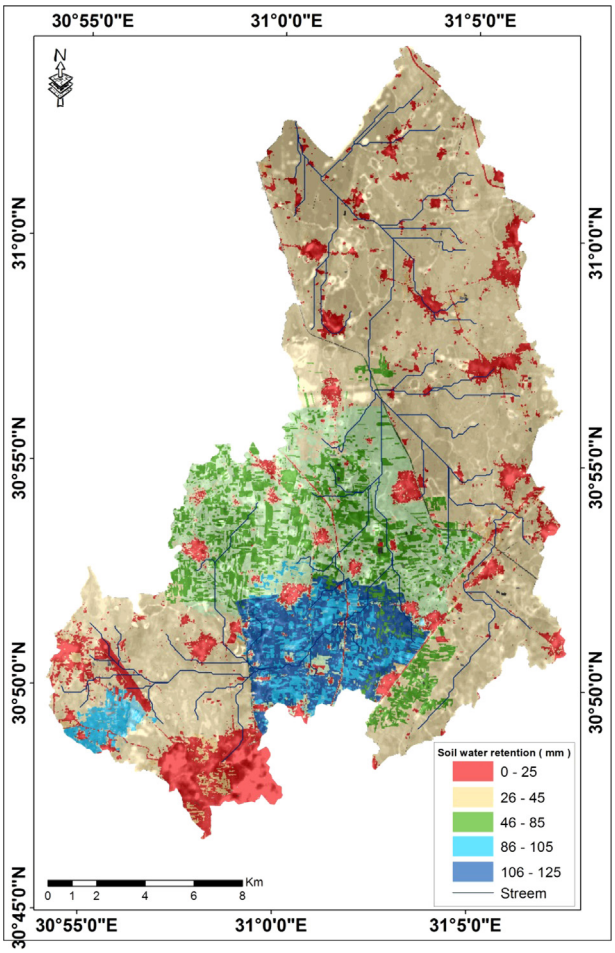

Fig. 6. Spatial distribution of soil water retention at catchment scale.

(*S*) varies between 26 and 45 mm. The results showed that areas with higher soil water retention are those falling in cropland-use far from the urban areas (Fig.6). Likewise, areas of lower soil water retention potential (0–25 mm) overlapped with areas of bare soils that are close to the urban area where water requirements are lower and higher soil dry bulk density values.

4. Discussion

Changes in LULC occur as an abrupt change with severe changes in soil properties. Due to the development and urbanization activity, soil infiltration capacity decreased and consequently land degradation increased (Abu-Hashim, 2011). These findings are in accordance with Mohamed and Belal (2015) that the strong trend of urban sprawl by building industrial was the main phenomena since there has been a strong reconstruction and urbanization in middle Nile Delta. Thus, changes in land-use have various impacts on soil infiltration capacity and its potential water retention through their impacts on soil water retention characteristics and the changes of soil pore distribution (Wahl, Bens, Schäfer, & Hüttl, 2003). With changing land-use and increasing urbanization activity within Tanta area from 1990 to 2015, total water storage capacity was decreased by 118.1 m^3 water per hectare, and these results are consistent with several authors (Hartge, 1988; Wahren, Feger, Schwärzel, & Münch, 2009; Abu-Hashim, 2011) who reported that deforestation, urbanization, and other land-use activities can significantly postpone the seasonal and annual distribution of surface flow and decrease the infiltration capacity. In addition, the contribution of cropland to the total water storage capacity was reduced through 1990–2015. This change in land use would affect the soil

physical, chemical, and biological characteristics, which influences the soil infiltration capacity (Wood & Blackburn, 1981; Shukla, Lal, Owens, & Unkefer, 2003; Fu et al., 2000). Furthermore, increases in ground cover resulted in increased soil water storage capacity (Gifford & Hawkins, 1978), and this concept was inconsistent with the investigated results. The results confirm that top soil conditions in cropland are favorable for enhancing infiltration (Fig. 6). Spatial distribution of soil water retention at the investigated area indicated that the highest values were associated with the particle-size distribution. In addition, DEM was used to describe the effects of slope variables on water retention and to assess the proportion of variation in soil water storage capacity (Chen et al., 2012). These results correspond well to the findings of Hartge (1988) that land-use changes consider the most representative parameter on soil infiltration and changes in infiltration capacity were initiated due to the effect of the land-use systems on soil properties. The most representative impact on the infiltration capacity in Tanat catchment is the loss of infiltrating area (cropland). During the 25 years between 1990 and 2015, 5300 ha of land was lost. This equals to 15 % of the total area of the whole catchment. The highest infiltration capacity observed in the cropland was due to improved soil characteristics as well as higher proportions of soil macro-pores that would be produced by the root activity compared to the urban areas (Mapa and Gunasena, 1995; Wahren et al., 2009), that are convenient well with the lowest values of soil dry bulk density at the study area. Spatial distributions (*S)* are mainly identified by the spatial heterogeneousness of LULC and soil types of the areas that are represented by the combination of the CN values (Hawkins et al., 2009) with different land-uses. Thus, areas with higher soil water retention (106–125 mm) are those that fall far from the urban areas which have lower values of soil dry bulk density and higher soil hydraulic conductivity (Wood & Blackburn, 1981; Hartge, 1988; Abu-Hashim, 2011).

5. Conclusion

Understanding how land-use influences water storage capacity of soils at the catchment scale enables formulating policies to reduce undesirable effects of land-use and land-management changes. Land-use changes (e.g. urbanization) enhanced impervious ground surfaces, decreasing soil water storage capacity, and increasing the tendency of land degradation. Integrating remote sensing, GIS and spatial hydrologic modeling (NRCS-CN model) could be used to identify essential inputs for precision water management to understand the reactions of arid ecosystems and to support the estimation of returning water benefits under such conditions. This study provides essential spatial distribution about soil water storage capacity as inputs for precision water management that is imperative on the Egyptian policies to perform swift and distinct techniques for implementing water conservation and mitigating water scarcity.

References

Abu-Hashim, M. S.D. (2011). *Impact of land-use and land management on water infiltration capacity on a catchment scale (PhD thesis)*. Germany: Fakultat Architektur Bauingeniurwesen und Umweltwissenschaften der Technischen Universitat Carolo-Wilhelmina zu Braunschweig.

Brandt, J., & Thornes, J. B. (1996). *Mediterranean desertification and land use* (p. 554)Chichester: Wiley554.

Chen, D. A., Stow, D. A., & Gong, P. (2004). Examining the effect of spatial resolution and texture window size on classification accuracy: an urban environment case. *International Journal of Remote Sensing*, *25*(11), 2177–2192.

Chen, Y., Wang, B., Pollino, C., & Merrin, L. (2012). Spatial modelling of potential soil water retention under floodplain inundation using remote sensing and GIS. In *Proceedings of the international congress on environmental modelling and software managing resources of a limited planet, sixth biennial meeting*. Leipzig, Germany: International Environmental Modelling and Software Society (iEMSs).

Chow, V. T., Maidment, D. R., & Mays, L. W. (1988). *Applied hydrology*. New York: McGraw-Hill.

Drake, N. A., & Vafeidis, A. (2004). A review of European Union funded research into the monitoring and mapping of Mediterranean desertification. *Advances in Environmental Monitoring and Modelling*, *1*(4), 1–51.

Fu, B. J., Chen, L. D., Ma, K. M., Zhou, H. F., & Wang, J. (2000). The relationships between land use and soil conditions in hilly area of the Loess Plateau in northern Shaanxi, China. *Catena*, *36*, 69–79.

Geetha, K., Mishra, S. K., Eldho, T. I., Rastogi, A. K., & Pandey, R. P. (2008). SCS-CN-based continuous simulation model for hydrologic forecasting. *Water Resources Management*, *22*(2), 165–190.

Gifford, G. F., & Hawkins, R. H. (1978). Hydrological impact of grazing on infiltration. *Water Resources Research*, *14*, 305–313.

Hartge, H. K. (1988). The problem of compaction on agricultural lands. *Applied Geography and Development*, *32*, 44–50.

Hawkins, R. H. (1993). A symptotic determination of runoff curve numbers from data. *Journal of Irrigation and Drainage 15 E.-ASCE*, *119*(2), 334–345.

Hawkins, R. H., Ward, T. J., Woodward, D. E., & Van Mullem, J. A. (2009). *Curve number hydrology: State of the practice* (Rev. Ed.). Washington D.C., USA: U.S.D.A.

King, K. W., & Balogh, J. C. (2008). Curve numbers for golf course watersheds. *Transactions of the American Society of Agricultural and Biological Engineers*, *51*(3), 987–996.

Klute, A. (1986). Water retention: Laboratory methods. In Klute, A. (Ed). Methods of soil analysis. Part 1. 2nd edition. *Agronomy monograph* (Vol. 9, pp. 635–662). Madison, WI: ASA and SSSA.

Kosmas, C., Danalatos, N. G., & Gerontidis, St (2000). The effect of land parameters on vegetation performance and degree of erosion under Mediterranean conditions. *Catena*, *40*, 3–17.

Kumar, P., Tiwari, K. N., & Pal, D. K. (1991). Establishing SCS runoff curve number from IRS digital database. *Journal of the Indian Society of Remote Sensing*, *19*(4).

Latha, M., Rajendran, M., & Murugappan, A. (2012). Comparison of GIS based SCS-CN and strange table method of rainfall-runoff models for Veeranam Tank, Tamil Nadu, India. *International Journal of Scientific Engineering Research*, *3*(10).

Lyon, S. W., Walter, M. T., Gerard-Marchant, P., & Steenhuis, T. S. (2004). Using a topographic index to distribute variable source area runoff predicted with the SCS curve–number equation. *Hydrological Processes*, *18*(15), 2757–2771.

Mantey, S., & Tagoe, N. D. (2013). Spatial modelling of soil conservation service curve number grid and potential maximum soil water retention to delineate flood prone areas: A case study. *Research Journal of Environmental and Earth Sciences*, *5*(8), 449–456.

Mapa, R. B., & Gunasena, H. P.M. (1995). *Effect of alley cropping on soil aggregate stability of a tropical Alfisol*. 32. Netherlands: Kluwer Academic Publishers, Agroforestry Systems237–245.

Michel, C., Andr´easSian, V., & Perrin, C. (2005). Soil conservation service curve number method: How to mend a wrong soil moisture accounting procedure?. *Water Resource Research*, *41*, W02011, http://dx.doi.org/10.1029/2004WR003191.

Ministry of Water Resources and Irrigation Egypt (MWRIE) (2014). *Water scarcity in Egypt*. Report 1–5 ⟨http://www.mfa.gov.eg/Site Collection Documents/Egypt %20 Water % 20 Resources %20 Paper_2014.pdf⟩.

Mishra, S. K., & Singh, V. P. (2006). A relook at NEH-4 curve number data and antecedent moisture condition criteria. *Hydrological Processes*, *20*(13), 2755–2768.

Mishra, S. K., Geetha, K., Rastogi, A. K., & Pandey, R. P. (2005). Long-term hydrologic simulation using storage and source area concepts. *Hydrological Processes*, *19*(14), 2845–2861.

Mohamed, E. S., Belal, A. (Dec. 15–16, 2015). Assessment of urban sprawl impact on agricultural land using remote sensing and GIS techniques. In *Proceedings of the soil international day conference*. Zagazig.

Mountrakis, G., Im, J., & Ogole, C. (2011). Support vector machines in remote sensing: a review. *ISPRS Journal of Photogrammetry and Remote Sensing*, *66*(3), 247–259.

Ponce, V. M., & Hawkins, R. H. (1996). Runoff curve number: has it reached maturity?. *Journal of Hydrology E.-ASCE*, *1*(1), 11–18.

Romero, P., Castro, G., Gomez, J. A., & Fereres, J. A. (2007). Curve number values for olive orchards under different soil moisture management. *Soil Science Society of America Journal*, *71*(6), 1758–1769.

Saxton, K. E., Rawls, W. J., Romberger, J. S., & Papendick, R. I. (1986). Estimating generalized soil–water characteristics from texture. *Soil Science Society of America Journal*, *50*, 1031–1036.

Sharma, K. D. (1998). The hydrological indicators of desertification. *Journal of Arid Environments*, *39*, 121–132.

Shukla, M. K., Lal, R., Owens, L. B., & Unkefer, P. (2003). Land use and management impacts on structure and infiltration characteristics of soils in North Appalachian region of Ohio. *Soil Science*, *168*, 167–177.

Singh, P. K., Bhunya, P. K., Mishra, S. K., & Chaube, U. C. (2008). A sediment graph model based on SCS-CN method. *Journal of Hydrology*, *349*(1–2), 244–255.

Soil Conservation Service, (1972). *SCS National engineering handbook, Section 4: Hydrology*. USDA.

SCS—Soil Conservation Service (1986). *National engineering handbook*, *Section 4, Hydrology*, Rev. Ed., Washington. D.C., USA: USDA.

Soulis, K., & Dercas, N. (2007). Development of a GIS-based spatially distributed continuous hydrological model and its first application. *Water International*, *32*(1), 177–192.

Thornes, J. B. (1985). The ecology of erosion. *Geography*, *70*, 222–234.

USDA, Natural Resource Conservation Service (2004). *National engineering handbook, Part 630, Hydrology* (Online). USA. To be found at ⟨www.wcc.nrcs.usda.gov/hydro/hydro-techref-neh-630.html⟩ (cited 10.01.10).

Wahl, N. A., Bens, O., Schäfer, B., & Hüttl, R. F. (2003). Impact of change in land-use management on soil hydraulic properties: hydraulic conductivity, water repellency and water retention. *Physics and Chemistry of the Earth*, *28*, 1377–1387.

Wahren, A., Feger, K. H., Schwärzel, K., & Münch, A. (2009). Land-use effects on flood generation-considering soil hydraulic conductivity measurements in modeling. *Advances in Geosciences*, *21*, 99–107.

Wood, M. K., & Blackburn, W. (1981). Grazing systems: their influence on infiltration rates in the rolling plains of Texas. *Journal of Range Management*, *34*, 331–335.

Zhan, X., & Huang, M. (2004). Arc CN-runoff: An Arc GIS tool for generating curve number and runoff maps. *Environmental Modelling and Software*, *19*(10), 875–879.